Two-loop $O(G_F M_H^2)$ radiative corrections to the Higgs boson decay width $H \to \gamma\gamma$ for large Higgs boson masses

J. G. Körner, K. Melnikov, and O. I. Yakovlev*
Institut für Physik, THEP, Johannes Gutenberg Universität, Staudinger Weg 7, D 55099 Mainz, Germany
(Received 25 September 1995)

This paper is devoted to the calculation of the two-loop $O(G_F M_H^2)$ radiative corrections to the Higgs boson decay width $H \to \gamma\gamma$ for large values of the Higgs boson mass M_H within the minimal standard model. The use of the equivalence theorem makes it possible to reduce the problem to the consideration of the physical Higgs boson field and the Goldstone bosons w^+, w^-, z. We present analytical results for the various two- and three-particle absorptive parts of the two-loop contributions, and, using dispersive techniques, analytic results for all but one of the dispersive contributions. The relative corrections to the decay width are large because of strong cancellations between the W and top loops in the lowest order, but the absolute corrections are small and perturbatively under control.

PACS number(s): 14.80.Bn, 12.15.Lk

I. INTRODUCTION

The neutral scalar Higgs boson is the essential ingredient of the standard model of the electroweak interactions. The Higgs boson mass is a free parameter in the minimal standard model and until now we did not know much about its value. Experiments exclude a Higgs boson lighter then ~ 65 GeV [1]. Also theoretical arguments based on perturbative unitarity suggest that the upper bound on the Higgs boson mass[1] is ~ 1 TeV [2].

It is widely believed that the properties of the Higgs boson can be investigated at the Next Linear Collider which will be able to operate in different modes $(e^+e^-, e^{+(-)}\gamma, \gamma\gamma)$. In particular, $\gamma\gamma$ collisions are well suited not only for the observation of the Higgs boson signal but also for studying its properties (for a review see Ref. [4]).

As is known for a long time, the $H\gamma\gamma$ vertex serves as a "counter" of the particles with masses larger than the Higgs boson mass: if these particles acquire masses because of the standard Higgs mechanism, then they do not decouple from the Higgs boson and provide a constant contribution to the $H\gamma\gamma$ vertex. Therefore, the $H\gamma\gamma$ vertex can provide us, in principle, with unique information about the structure of the theory at energy scales unachievable at modern accelerators.

A similar consideration also shows up in another aspect: it turns out that the $H\gamma\gamma$ vertex is very sensitive to different anomalous couplings in the massive gauge boson sector of the standard model (SM). All these properties make the $H\gamma\gamma$ interaction vertex an extremely interesting object from the theoretical point of view. In order to exploit the possibility of looking for deviations from the SM predictions for the $H\gamma\gamma$ vertex, one needs quite accurate predictions for this vertex within the framework of the minimal standard model.

At the tree level, the $H\gamma\gamma$ vertex is absent in the standard model. At the one-loop level, the W boson and the top quark contribute to the effective $H\gamma\gamma$ form factor. The one-loop result was obtained in Refs. [5,6] and can be found in the text books [7]. Note for the time being that the contributions of the W and t-quark loop to the $H\gamma\gamma$ vertex have different signs and hence tend to compensate each other. For realistic masses of the W boson and the top quark, this compensation occurs for Higgs boson masses of ~ 600 GeV.

The QCD radiative corrections to the $H\gamma\gamma$ vertex were calculated recently by several groups [8]. These corrections are negligible below $t\bar{t}$ threshold and are large above the threshold. As for the size of the other SM radiative corrections, we do not know much about them at present. Recently, the corrections of order $O(G_F m_t^2)$ were evaluated in the limit of a small Higgs mass [9]. In this paper we consider the leading $O(G_F M_H^2)$ SM radiative corrections in the limit of large Higgs boson masses. We show that this correction has the same order of magnitude but has the opposite sign as the QCD correction in the interval $0.5\ \text{TeV} < m_H < 1.5$ TeV and blows up for larger Higgs boson masses.

The technical tool which results in great simplifications of the calculations is the use of the Goldstone boson equivalence theorem (ET) [10].

The organization of the paper is as follows: in Sec. II we discuss the one-loop calculation of the $H\gamma\gamma$ vertex in the framework of the ET; Sec. III is devoted to the two-loop calculation: we briefly discuss the renormalization procedure and present results for the imaginary and real parts of the $H\gamma\gamma$ vertex; in Sec. IV we discuss our final results and make some concluding remarks.

II. LOWEST ORDER $H\gamma\gamma$ VERTEX

The interaction of the Higgs boson with two photons can be described with the help of the effective Lagrangian

$$L = \frac{\alpha}{4\pi v} F(s) F_{\mu\nu} F^{\mu\nu} H. \tag{1}$$

In this equation, $F(s)$ denotes a form factor which contains all information about the particles propagating in the

*Permanent address: Budker Institute for Nuclear Physics, 630 090, Novosibirsk, Russia.

[1]This statement is also supported by lattice investigations [3].

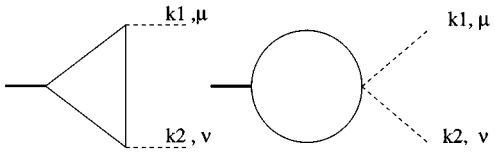

FIG. 1. Generic lowest order graphs. The dashed lines correspond to photons, heavy solid lines are Higgs bosons. The particles inside the loop (light solid lines) are W bosons and top quarks.

loop. In the minimal standard model, the form factor $F(s)$ obtains contributions from the top quark and the W boson.

The lowest order contribution to the $H\gamma\gamma$ vertex is given by the graphs shown in Fig. 1. The analytical results for the fermion and spin-one boson contributions can be found, e.g., in [7]. In the limit when the Higgs boson mass is large in comparison with the mass of the particle propagating in the loop, the contribution of the fermions to $F(s)$ is suppressed as $(M_f/M_H)^2$, while the contribution of the W loop results in a constant

$$F^{(0)}_{m_H\to\infty}\to 2. \tag{2}$$

This asymptotic value can be obtained using the Goldstone boson equivalence theorem which states that in the limit of a large Higgs boson mass $M_H \gg M_W$, the leading $O(G_F M_H^2)$ contribution to a given Green's function can be obtained by replacing the gauge bosons W,Z by the corresponding would-be Goldsone bosons w,z of the symmetry-breaking sector of the theory. The Goldstone bosons can be taken to be massless in this approximation [10].

The interaction of the would-be Goldstone bosons with the Higgs and photon fields is described by the $U_{\rm EM}(1)$ gauged linear σ model:

$$L=(D_\mu w)^*(D^\mu w)+\frac{1}{2}\partial_\mu z\partial^\mu z+\frac{1}{2}\partial_\mu H\partial^\mu H-\frac{1}{2}M_H^2H^2 - \frac{M_H^2}{4v^2}(\Phi^2+H^2)^2-\frac{M_H^2}{v}(\Phi^2+H^2)H-\frac{1}{4}F_{\mu\nu}F^{\mu\nu}. \tag{3}$$

Here $D_\mu=\partial_\mu-ieA_\mu$ is the $U_{\rm EM}(1)$ covariant derivative, M_H is the mass of the Higgs boson field, v is its vacuum expectation value, and Φ is the triplet of the Goldstone bosons w^+,w^-,z. The Feynman rules for this Lagrangian can be found, e.g., in Ref. [11].

Let us first reproduce the result of Eq. (2) using the Lagrangian of Eq. (3). It is straightforward to write down the sum of the Feynman graphs shown in the Fig. 1 (neglecting for the moment the contribution from the top loop). The contribution to the form factor $F(s)$ can be conveniently obtained by contracting the one-loop tensor amplitude with the tensor (the notation for outgoing photons is clarified in Fig. 1):

$$d^{\mu\nu}=g^{\mu\nu}k_1k_2-k_1^\nu k_2^\mu. \tag{4}$$

In spite of the fact that the sum of these graphs should be ultraviolet finite, we need to regularize at intermediate steps of the calculation. For simplicity, we adopt dimensional regularization, working in d dimensions. At the end of the calculations we shall put d equal to four. After some algebra one finds for the sum of the lowest order amplitudes:

$$M=M_{\mu\nu}d_{\mu\nu}=M_H^2 2\pi\alpha(d-4)s \times\int\frac{d^dq}{(2\pi)^d}\frac{1}{(k_1+q)^2(k_2-q)^2}. \tag{5}$$

From this equation it is seen that the leading order calculation amounts to the calculation of the divergent part of the massless two-point function. Using well-known results for the two-point function in Eq. (5), we obtain the asymptotic result given in Eq. (2).

It is also possible to calculate these graphs using dispersion relations. In order to do this, we need to cut the graphs shown in Fig. 1 in all possible ways, calculate the contribution of the cut graphs to the imaginary part of the $F(s)$ using unitarity and finally integrate the imaginary part of the $F(s)$ along the cut. As our Goldstone bosons are exactly massless, the cut goes from 0 to ∞ in the complex s plane. If we cut the graphs of Fig. 1, the imaginary part of $F(s)$ is given by the convolution of the decay amplitude $H(s)\to w^+w^-$, with the amplitude $w^+w^-\to\gamma\gamma$. Note that conservation of the total angular momentum requires equal helicities of both photons in the final state.

It is not difficult to see by exact calculation that the amplitude $w^+w^-\to\gamma\gamma$ vanishes for massless w^+ and w^- bosons in the equal photon helicity configuration. Therefore, the imaginary part of the $F(s)$ is zero and one fails to reproduce the result of the direct evaluation of the Feynman graphs. To find a way out of this paradox, we need to investigate the amplitude $w^+w^-\to\gamma\gamma$ more carefully. For this aim we introduce a mass for the Goldstone bosons which now serves as an infrared cutoff. The amplitude is then

$$d^{\mu\nu}M_{\mu\nu}(w^+w^-\to\gamma\gamma)=ie^2\frac{2m^2s^2}{(t-m^2)(u-m^2)}, \tag{6}$$

where m is the mass of the Goldstone bosons and t and u are the Mandelstam variables of the process.

It is then straightforward to calculate the imaginary part of the $F(s)$ to the lowest order. One obtains

$$\mathrm{Im}F^{(0)}(s)=-\pi M_H^2\frac{4m^2}{s^2}\ln\left(\frac{1+\beta}{1-\beta}\right), \tag{7}$$

where β is the velocity of the (massive) Goldstone boson. If we put the mass of the Goldstone boson equal to zero in Eq. (7), the imaginary part of $F(s)$ is zero in accordance with the previous statement. However, the lower limit in the dispersion integral is $4m^2$. In fact, if we consider the imaginary part given by Eq. (7) in the dispersion integral, we can see that in the limit $m\to 0$, the imaginary part of $F(s)$ turns into a δ(s) function.

Hence, the correct procedure consists in evaluating the dispersion integral with finite Goldstone boson masses and taking the limit $m\to 0$ only after the integration over the cut has been performed.

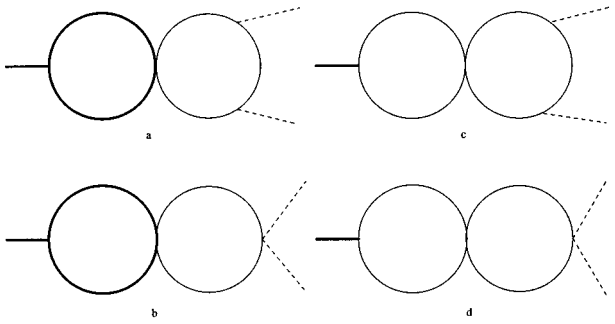

FIG. 2. "Quasi one-loop," two-loop diagrams. Heavy solid lines denote Higgs bosons, thin solid lines denote w^+, w^-, z Goldstone bosons of the ET. Dashed lines are photons.

In this way, we obtain the same result as in Eq. (2) for the real part of $F(s)$, as has been obtained from the known complete expression for $F(s)$ in the large Higgs boson mass limit or from the direct evaluation of the Feynman graphs with massless Goldstone bosons.

The reason why we have discussed the one-loop calculation of the $H\gamma\gamma$ vertex in some detail is twofold: first, it serves as a reference point to justify the use of the equivalence theorem for the two-loop calculation; second, in our opinion, this calculation shows some unexpected properties. (For instance, the evaluation of this one-loop result through the dispersion relations is very similar to the evaluation of the axial anomaly through the imaginary part of the triangle graph [12]. However, we have not succeeded in finding any deep reason underlying this similarity.)

III. TWO-LOOP CONTRIBUTION TO THE $H\gamma\gamma$ VERTEX

A. Renormalization

In this subsection we briefly discuss the renormalization procedure which is needed for the evaluation of the two-loop graphs. First note that as the $H\gamma\gamma$ interaction is absent in the SM Lagrangian, the two-loop graphs must be finite after we renormalize all subdivergencies. In other words, to make our two-loop amplitude finite, we need only one-loop counter terms. The latter are constructed according to the following procedure.

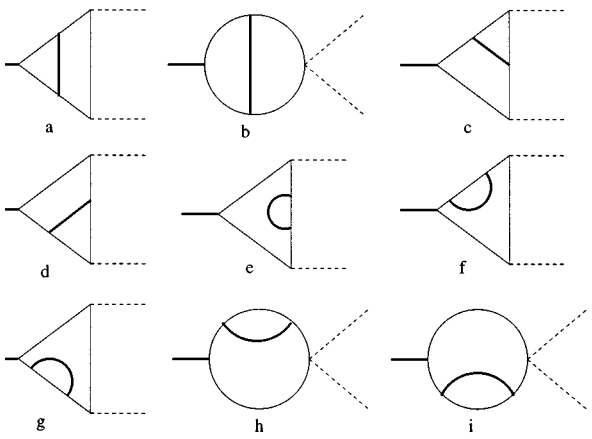

FIG. 3. Abelian (QED-like) two-loop diagrams. Line drawings as in Fig.2.

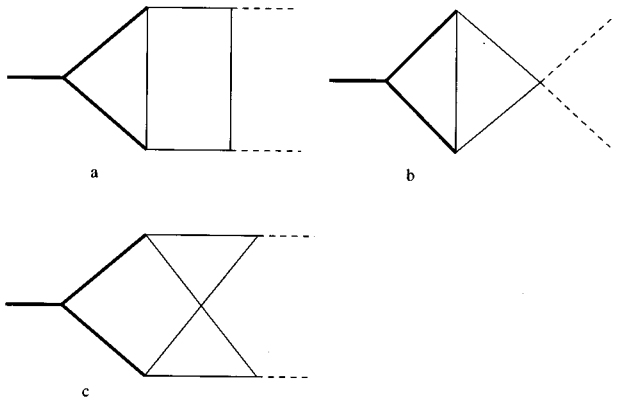

FIG. 4. Two-loop diagrams with triple Higgs boson couplings. Line drawings as explained in Fig. 2.

The "matter" part of the Lagrangian [Eq. 3] contains two independent parameters: the mass of the Higgs boson field M_H and the vacuum expectation value v. We fix the one-loop counter terms by requiring the mass of the Higgs boson field and the vacuum expectation value to be exact one-loop quantities. This requirement eliminates all tadpole graphs and provides us with the counter terms for all other divergent subgraphs. For instance, the self-energies of the Goldstone bosons must be effectively subtracted on mass shell. Further, we will need the counter terms for the vertices Hw^+w^- and Hzz which can also be obtained from the above requirements.

The next point is the renormalization of the $\gamma w^+ w^-$ vertex. As this vertex is convergent, its renormalization is fixed by the renormalization of the Goldstone boson wave function which in turn is fixed by the renormalization of the self-energy operator for the Goldstone boson. This procedure is compatible with the electromagnetic Ward identities of the gauged σ model.

B. Two-particle cuts

In this subsection we compute the contributions of the two-particle cuts of the graphs presented in Figs. 2–5. The simplest (quasi one-loop) contributions are given by the set of Feynman graphs shown in Fig. 2 and the two-particle cuts of the graphs in Fig. 5.

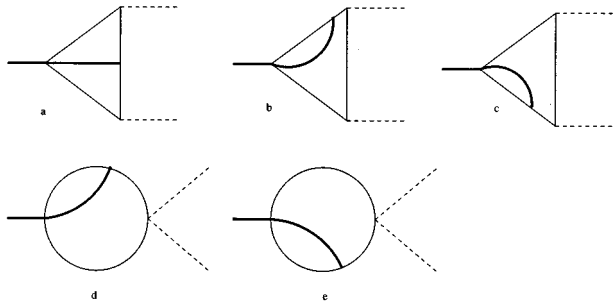

FIG. 5. Two-loop diagrams with two-Higgs-boson–two-Goldstone-boson interaction vertices.

The graphs shown in Fig. 2 are quasi one-loop graphs. As the Hw^+w^- vertex diverges at the one-loop level, one needs to bring in counter terms which can be obtained according to the recipe given above. It is also convenient to consider simultaneously the graphs shown in Fig. 2 and the two-particle cuts of the two-Higgs-two Goldstone boson vertex graphs presented in Fig. 5. Summing up the contributions of Fig. 2, the two-particle cut contributions of the graphs shown in Fig. 5 and the one-loop counter term for the Hw^+w^- vertex, one has

$$F^{(1)}=2\left(\frac{M_H}{4\pi v}\right)^2(2-\sqrt{3}\pi). \tag{8}$$

Next, we discuss the contribution of the graphs shown in Fig. 3. Note that we are considering only two-particle cuts in this section.

Let us start with the graphs shown in Figs. 3(a) and 3(b) and consider the two-particle cuts which lie to the right of the virtual Higgs boson line. The cut contribution is given by the convolution of the one-loop $H\to w^+w^-$ amplitude (with the Higgs boson in the t channel) with the Born amplitude for $w^+w^-\to\gamma\gamma$. As we know from the discussion of the lowest order vertex, the latter is singular for small values of s. Unfortunately, the one-loop correction to $H\to w^+w^-$ is also singular for $s=0$ if the Goldstone bosons are exactly massless. As before, we have to introduce a mass m for the Goldstone boson to handle this infrared divergence. Note at this point that the ET guarantees the existence of a smooth limit as $m\to 0$. Hence, we expect that the sum of all two-loop contributions will not be sensitive to the details of the infrared limit of the theory.

Evaluating the Hw^+w^- vertex in the limit $m_H>>\sqrt{s},m$ we find the result

$$F_L=\frac{M_H^2}{2}\left(\frac{M_H}{4\pi v}\right)^2\left[1+\ln\left(\frac{M_H^2}{m^2}\right)-\beta\ln\left(\frac{1+\beta}{1-\beta}\right)\right]. \tag{9}$$

Putting everything together, the imaginary part corresponding to the "right cut" graphs of Figs. 3(a) and 3(b) is given by

$$\mathrm{Im}F^{(2)}=-\frac{M_H^2}{2}2\pi\frac{4m^2}{s^2}\ln\left(\frac{1+\beta}{1-\beta}\right)F_L(s). \tag{10}$$

Inserting Eq. (10) into a dispersion integral, we can evaluate the contribution of these cut graphs to the real part of the $F(s)$ and get

$$F^{(2)}=2\left(\frac{M_H}{4\pi v}\right)^2\left[1+\ln\left(\frac{M_H^2}{m^2}\right)-\frac{4}{3}\left(1+\frac{\pi^2}{12}\right)\right]. \tag{11}$$

Another possibility to cut the graphs of Figs. 3(a) and 3(b) is to cut to the left of the virtual Higgs boson line. We divide the integration region in the dispersion integral into two parts, introducing an arbitrary scale μ. The scale μ can be chosen to satisfy the inequalities

$$m\ll\mu\ll M_H.$$

If we are interested in the contribution from the "high-energy" part of this graph, we can put the masses of the Goldstone bosons equal to zero. For the "high-energy" part of the imaginary part of $F(s)$, we obtain

$$\mathrm{Im}F_h^{(3)}=-\frac{M_H^4}{2}\left(\frac{M_H}{4\pi v}\right)^2\frac{\pi}{s^3}A,$$

$$A=\left[8s-4(s+M_H^2)\ln\left(\frac{s+M_H^2}{M_H^2}\right)+4M_H^2\mathrm{Li}_2\left(-\frac{s}{M_H^2}\right)\right]. \tag{12}$$

In this equation, $\mathrm{Li}_2(x)$ is a Spence function as, e.g., defined in Ref. [13]. Inserting this expression into the dispersion integral, we can evaluate the contribution of the "high-energy" part to the real part of $F(s)$, where we must remember that the lower limit for the integration of the above quantity is given by μ.

Performing the integration, we get

$$F_h^{(3)}=2\left(\frac{M_H}{4\pi v}\right)^2\left[\frac{1}{4}\ln\left(\frac{\mu^2}{M_H^2}\right)-\frac{7}{2}+\frac{\pi^2}{6}+\frac{3}{2}\zeta(3)\right]. \tag{13}$$

Next, we have to find the contribution of the "low-energy" region of these graphs to $F(s)$. We do this by expanding the amplitude in terms of powers of $\sqrt{s}/M_H$ and m/M_H.

The result for the imaginary part reads

$$\mathrm{Im}F_l^{(3)}=-\pi M_H^2\left(\frac{M_H}{4\pi v}\right)^2\frac{\beta}{s^2}\left[-\frac{s}{2}+4m^2\left(\frac{\pi^2}{2}-\ln^2\frac{1+\beta}{1-\beta}\right)\right]. \tag{14}$$

Inserting (14) into the dispersion integral and integrating from $4m^2$ up to μ^2, we find the "low-energy" contribution to the real part of $F(s)$:

$$F_l^{(3)}=2\left(\frac{M_H}{4\pi v}\right)^2\left(-\frac{1}{4}\ln\frac{\mu^2}{m^2}-\frac{5}{6}+\frac{\pi^2}{18}\right). \tag{15}$$

Finally, we have to sum the "low-energy" and "high-energy" contributions and get

$$F^{(3)}=2\left(\frac{M_H}{4\pi v}\right)^2\left(-\frac{1}{4}\ln\frac{M_H^2}{m^2}-\frac{13}{3}+\frac{\pi^2}{9}+\frac{3}{2}\zeta(3)\right). \tag{16}$$

The next two-particle cut contributions that we have to consider are obtained by cutting the graphs presented in Figs. 3(c)–3(e). The calculation proceeds in complete analogy with the case considered in detail above. The result of our evaluation is

$$F^{(4)}=2\left(\frac{M_H}{4\pi v}\right)^2\left(-\frac{3}{4}\ln\frac{M_H^2}{m^2}-\frac{\pi^2}{2}+\frac{3}{2}\zeta(3)+3\right). \tag{17}$$

We mention that the graphs in Figs. 3(f)–3(i) have no two-particle cuts because of using on-shell renormalization for the Goldstone bosons.

If we sum $F^{(2)}$, $F^{(3)}$, and $F^{(4)}$, we see that the sum is finite in the limit $m\to 0$ in agreement with our expectations:

$$F^{(2)}+F^{(3)}+F^{(4)}=2\left(\frac{M_H}{4\pi v}\right)^2\left(3\zeta(3)-\frac{\pi^2}{2}-\frac{5}{3}\right). \quad (18)$$

To recapitulate, Eq. (18) contains the contributions of the two-particle cuts of the diagrams in Fig. 3.

Next we are going to discuss the two-particle cut contributions corresponding to the graphs presented in Figs. 4(a) and 4(b). Similar to the situation discussed above there are two possible ways of cutting these graphs, i.e., to the left and to the right of the virtual Goldstone boson line.

We start with the contribution of the right-cut graph. Its contribution is given by the convolution of the correction to the Hw^+w^- vertex and the $w^+w^-\to\gamma\gamma$ amplitude. In this case, the Hw^+w^- vertex is not singular for $s=0$ when the Goldstone bosons are massless. Hence, the contribution of this ''right-cut'' graph is simply given by the product of the lowest order $w^+w^-\to\gamma\gamma$ amplitude and the Hw^+w^- vertex calculated for $s=0$. One obtains

$$F^{(5)}=2\left(\frac{M_H}{4\pi v}\right)^2 3. \quad (19)$$

The contributions of the ''left-cut'' graphs are also calculated straightforwardly.[2] After a little algebra, we find the result for the imaginary part

$$\mathrm{Im}F^{(6)}=\frac{3\pi}{2}\left(\frac{M_H}{4\pi v}\right)^2\frac{M_H^4}{s^2}2\beta_H\left[\frac{1+\beta_H^2}{\beta_H}\ln\left(\frac{1+\beta_H}{1-\beta_H}\right)-2\right]. \quad (20)$$

In this equation

$$\beta_H=\sqrt{1-\frac{4M_H^2}{s}}$$

is the velocity of the Higgs boson in the intermediate state. Note, that the dispersion integral starts at the point $s=4M_H^2$. The result of the integration is given by:

$$F^{(6)}=2\left(\frac{M_H}{4\pi v}\right)^2\left(\sqrt{3}\pi-\frac{\pi^2}{6}-\frac{15}{4}\right). \quad (21)$$

The next step is the evaluation of the contribution of the graph presented in Fig. 4(c). There is only one possibility to obtain a two-particle cut from this graph, it is the cut with the two Higgs bosons in the intermediate state. The evaluation of this cut is much more involved because of its nonplanar topology. Some details of our evaluation of this graph are given below.

First, after cutting the graph, we face the necessity for evaluating the box graph. Contracting the box amplitude with the $d_{\mu\nu}$ tensor [defined in Eq. (4)], we find the representation for the box graph contribution

$$T_{\mu\nu}d_{\mu\nu}=\frac{i}{(4\pi)^2}\int dydz\left(\frac{2s}{g(y,z)}+\frac{-sm^2+(M_H^2-t)(M_H^2-u)}{g^2(y,z)}\right), \quad (22)$$

where s,t,u are the usual Mandelstam variables and the function $g(y,z)$ reads

$$g(y,z)=m^2+(u-m^2)y+(t-m^2)z+syz.$$

The y and z integrations in Eq. (22) extend from 0 to 1. After integration over y and z, we get the result for the box graph amplitude

$$M=4\pi\alpha i\left(\frac{M_H}{4\pi v}\right)^2 2\left[\ln^2\left(\frac{tu-M_H^4}{(t-M_H^2)(u-M_H^2)}\right)-4\mathrm{Li}_2(1)+2\mathrm{Li}_2\left(\frac{tu-M_H^4}{(t-M_H^2)(u-M_H^2)}\right)+\mathrm{Li}_2\left(-\frac{(t-M_H^2)^2}{tu-M_H^4}\right)+\mathrm{Li}_2\left(-\frac{(u-M_H^2)^2}{tu-M_H^4}\right)+\frac{1}{2}\ln\left(\frac{-tu}{M_H^4}\right)\right]. \quad (23)$$

To calculate the contribution of the box to the imaginary part of the $F(s)$, we have to integrate Eq. (23) over two-particle phase space. In doing so, it is convenient to introduce a new variable $0<x<1$ according to

$$\frac{s}{M_H^2}=\frac{(1+x)^2}{x}. \quad (24)$$

Then, the contribution of the box to the imaginary part of the $F(s)$ is given by

$$\mathrm{Im}F^{(7)}=-2\times\frac{3}{2}\left(\frac{M_H}{4\pi v}\right)^2\frac{M_H^4}{s^2}\left[\frac{1-x}{1+x}\left(2\ln^2(x)-2\frac{1+x^2}{1-x^2}\ln(x)-2\pi^2-2\right)+8\mathrm{Li}_2(-x)+2\frac{\pi^2}{3}-2\ln^2(x)+8\ln(x)\ln(1+x)\right]. \quad (25)$$

Finally, in order to obtain its contribution to the real part of $F(s)$, one needs to integrate the imaginary part along the cut. It is clear from the graph in Fig. 4(c) that the cut goes from $4M_H^2$ to ∞. Performing this calculation, we find

$$F^{(7)}=-2\left(\frac{M_H}{4\pi v}\right)^2\frac{3}{2}\left(-\frac{4}{9}\zeta(3)+\frac{38}{27\sqrt{3}}\pi^3-\frac{23}{9}\pi^2+\frac{2}{\sqrt{3}}\pi-\frac{11}{6}+8C_1\right). \quad (26)$$

[2]There is one subtlety in this discussion. Considering this cut graph more carefully, we find both real and *imaginary* parts originating, e.g., from the imaginary part of the box graph $HH\to\gamma\gamma$. For our purposes, we need only the real part of the amplitude, which (after being integrated over the intermediate particle phase space in the unitarity relation) results in Eq. (20). As for the *imaginary* part of the box graph, it will be exactly canceled by the imaginary part of the *three-particle cut*. In the latter case, the imaginary part comes from the pole of the virtual Higgs boson propagator, which comes into play when the total energy of the process is larger than $2M_H$ [see also the discussion after Eqs. (38) and (39)].

Here, the constant C_1 is

$$C_1=\int_0^1 dx\,\frac{\ln(x)\ln(x^2+x+1)}{1+x}=-0.194\,692. \qquad (27)$$

The result in Eq. (26) completes the list of the two-particle cut contributions.

C. Three-particle cuts

This subsection is devoted to the discussion of the three-particle cuts. First, we consider the graphs corresponding to Figs. 3(f)–3(i). We remind the reader that these graphs have no two-particle cuts because of using on-shell renormalization for the Goldstone bosons. In order to evaluate the three-particle intermediate state contribution, we have to consider the convolution of the two processes $H\to w^+w^-H$ and $(Hw^+)w^-\to\gamma\gamma$. As indicated by the parentheses, the latter process can be viewed as the annihilation of a massless particle w^- and the massive particle (Hw^+) into two photons. It is not difficult to calculate the $d^{\mu\nu}$-contracted amplitude for $(Hw^+)w^-\to\gamma\gamma$ which reads

$$M^{\mu\nu}[(Hw^+)w^-\to\gamma\gamma]d_{\mu\nu}=ie^2\frac{M_H^2}{v}. \qquad (28)$$

It is then clear that the problem of the calculation of the imaginary part for this cut contribution amounts to the problem of averaging the virtual Goldstone boson propagator on the left side of this graph over three-particle phase space. Performing the integration, we find

$$\mathrm{Im}F^{(8)}=-\frac{M_H^4}{2}\left(\frac{M_H}{4\pi v}\right)^2\frac{2\pi}{s^3}\left[-2(s-M_H^2)+(s+M_H^2)\ln\left(\frac{s}{M_H^2}\right)\right]. \qquad (29)$$

We finally substitute this expression into the dispersion integral and integrate along the cut going from $s=M_H^2$ to $s=\infty$. The result of this integration is

$$F^{(8)}=2\left(\frac{M_H}{4\pi v}\right)^2\left(\frac{13}{8}-\frac{\pi^2}{6}\right). \qquad (30)$$

Next, we discuss the three-particle cuts of the graphs in Figs. 3(a) and 3(b). Cutting these graphs along the three-particle intermediate state contributions, it is easy to see that these graphs produce exactly the same result as the graphs discussed previously [Figs. 3(f)–3(i)].

A more nontrivial situation arises for the three-particle cut of the graphs shown in Figs. 3(c) and 3(d). In this case, the complexity stems from the fact that the amplitude to the right of the cut does not have a simple form as in Eq. (28). The way we proceed is the following: as before, we first contract this amplitude with the tensor $d_{\mu\nu}$, and then perform the phase space integration over the momentum of the decay products of the virtual Goldstone boson. Then, we obtain the representation for the imaginary part of $F(s)$

$$\mathrm{Im}F^{(9)}=-\frac{8\pi^2M_H^2}{s^2}\left(\frac{M_H^2}{v}\right)^2\int\frac{d^3p_2}{(2\pi)^3 2E_2}\frac{\Gamma_2(Q)}{Q^2}\times\left(\frac{s}{Qk_1}-1\right), \qquad (31)$$

where $Q=k_1+k_2-p_2$ and $\Gamma_2(Q)$ is given by

$$\Gamma_2(Q)=\frac{1}{8\pi}\frac{Q^2-M_H^2}{Q^2}.$$

Integrating Eq. (31), we obtain the result for the contribution of this graph to the imaginary part of $F(s)$

$$\mathrm{Im}F^{(9)}=-2\pi\left(\frac{M_H}{4\pi v}\right)^2\frac{M_H^4}{4s^3}A,$$

$$A=\left[2s\ln^2\left(\frac{s}{M_H^2}\right)-(6s+2M_H^2)\ln\left(\frac{s}{M_H^2}\right)+8(s-M_H^2)\right]. \qquad (32)$$

Integrating Eq. (32) along the cut, we finally obtain the contribution to the real part of $F(s)$, which reads

$$F^{(9)}=2\left(\frac{M_H}{4\pi v}\right)^2\frac{1}{4}\left(\frac{4\pi^2}{3}-\frac{17}{2}-4\zeta(3)\right). \qquad (33)$$

Next, we come to the discussion of the graphs shown in Fig. 5. The calculation is performed in complete analogy with the case discussed previously. Without going into details, we present the result for the imaginary and real parts of the corresponding cut graphs: the joint contribution of the cut graphs in Figs. 5(b) and 5(d) to the imaginary part is the same as the contribution of the cut graphs in Figs. 5(c) and 5(e) and it has the form

$$\mathrm{Im}F^{(10)}=-2\pi\left(\frac{M_H}{4\pi v}\right)^2\frac{M_H^2}{2s^3}\left[\frac{(s+M_H^2)(s-M_H^2)}{2}-sM_H^2\ln\left(\frac{s}{M_H^2}\right)\right]. \qquad (34)$$

Upon integration we get, for the real part

$$F^{(10)}=2\left(\frac{M_H}{4\pi v}\right)^2\left(\frac{\pi^2}{12}-\frac{7}{8}\right). \qquad (35)$$

Next, let us write down the contribution of the cut graph shown in Fig. 5(a):

$$\mathrm{Im}F^{(11)}=-2\pi\left(\frac{M_H}{4\pi v}\right)^2\frac{M_H^2}{4s^3}B,$$

$$B=\left[-2sM_H^2\ln^2\left(\frac{s}{M_H^2}\right)-2sM_H^2\ln\left(\frac{s}{M_H^2}\right)+(s-M_H^2)(3s-M_H^2)\right]. \qquad (36)$$

Correspondingly, one has, for the real part,

$$F^{(11)}=2\left(\frac{M_H}{4\pi v}\right)^2\frac{1}{4}\left(4\zeta(3)+\frac{\pi^2}{3}-\frac{17}{2}\right). \tag{37}$$

Next, we consider the contribution of the three-particle cuts of the graphs shown in Figs. 4(a) and 4(b). The first step of the calculation is similar to the evaluation of the graphs in Figs. 5(b)–5(e) because the right-hand side of the cut graph is again given by the simple expression Eq. (28). Performing all further integrations over the phase space variables, we obtain the representation for the imaginary part of the sum of these cut graphs

$$\mathrm{Im}F^{(12)}=-2\pi\left(\frac{M_H^2}{4\pi v}\right)^2\frac{6M_H^4}{s^2}\int_m^{E_{\max}}dE\,\frac{\sqrt{E^2-M_H^2}}{s-2\sqrt{s}E}, \tag{38}$$

where $E_{\max}$ is given by

$$E_{\max}=\frac{s+M_H^2}{2\sqrt{s}}. \tag{39}$$

One integrates over the energy of the virtual Higgs boson which decays to two Goldstone bosons. The specific feature of this integral is that, depending on the total energy of the process $\sqrt{s}$, the denominator of the integral can go through zero reflecting the fact that an intermediate state with two ''real'' Higgs bosons can be formed for $s>4M_H^2$. It is also clear that for our purposes we have to treat this singularity in the principal value sense.

It is straightforward to calculate this integral and one obtains the expression for the imaginary part

$$\mathrm{Im}F^{(12)}=-2\pi\left(\frac{M_H^2}{4\pi v}\right)^2\frac{6M_H^4}{s^2}\frac{1}{4}\left(-\frac{1}{2}\ln\frac{s}{M_H^2}-1+\frac{M_H^2}{s}+\Psi(s)\right), \tag{40}$$

where the function $\Psi(s)$ is defined by

$$\Psi(s)=\theta(4M_H^2-s)\frac{3}{2}\cot\left(\frac{\varphi}{2}\right)\left(\varphi-\frac{\pi}{3}\right)-\theta(s-4M_H^2)\frac{3}{2}\frac{1-x}{1+x}\ln(x). \tag{41}$$

The variable x is defined as in Eq. (24) and φ is defined through the relation

$$s=4M_H^2\sin^2\frac{\varphi}{2}.$$

Integrating the imaginary part, we finally obtain the contribution to the real part of $F(s)$

$$F^{(12)}=2\left(\frac{M_H}{4\pi v}\right)^2\left[\frac{\pi^2}{8}+\frac{3}{2}-\frac{3\sqrt{3}}{2}\mathrm{Cl}_2\left(\frac{\pi}{3}\right)\right], \tag{42}$$

where $\mathrm{Cl}_2(\varphi)$ is Clausen's function (see, e.g., [13]).

Now we are in the position to discuss the most difficult part of the calculation, namely, the evaluation of the contribution of the three-particle cut given by the nonplanar graph of Fig. 4(c). Performing the integration over phase space, we obtain the representation for the contribution of this cut to the imaginary part of $F(s)$

$$\mathrm{Im}F^{(13)}=-2\pi\left(\frac{M_H^2}{4\pi v}\right)^2\frac{6M_H^4}{s^2}[W_1(s)+W_2(s)+W_3(s)], \tag{43}$$

where W_1, W_2, and W_3 stand for

$$W_1(s)=2\left(2\ln(2)+\frac{1}{2}\right)\int_m^{E_{\max}}dE\,\frac{\beta_H E}{s-2\sqrt{s}E}, \tag{44}$$

$$W_2(s)=-2\int_m^{E_{\max}}\frac{dE}{\sqrt{s}}\,\frac{s-E\sqrt{s}}{s-2\sqrt{s}E}\ln\left(\frac{s-E\sqrt{s}+\beta_H E\sqrt{s}}{s-E\sqrt{s}-\beta_H E\sqrt{s}}\right), \tag{45}$$

$$W_3(s)=-2\int_m^{E_{\max}}dE\,\frac{\beta_H E}{s-2\sqrt{s}E}\ln\left(\frac{(s-E\sqrt{s})^2}{(\beta_H E\sqrt{s})^2}-1\right). \tag{46}$$

In this expression, $E_{\max}$ is defined through Eq. (39) and β_H is the velocity of the Higgs boson:

$$\beta_H=\sqrt{1-\frac{4M_H^2}{E^2}}.$$

In each of the above integrals, there is a pole in the integrand for total energies larger than twice the Higgs boson mass. We first evaluate each of these integrals in the case where $s>4M_H^2$ and then perform an analytic continuation to the region $s<4M_H^2$. We shall not present explicit expressions for the imaginary part of these functions above threshold. If needed, it can be obtained directly from the integral representation of the above functions. One obtains

$$\begin{aligned}W_1(s)+W_3(s)=&\frac{1}{4}\left(1-\frac{M_H^2}{s}\right)-\frac{1}{8}\ln\left(\frac{s}{M_H^2}\right)+\frac{1}{8}\ln^2\left(\frac{s}{M_H^2}\right)\\&-\frac{M_H^2}{2s}\ln\left(\frac{s}{M_H^2}\right)+\frac{1-x}{2(1+x)}\left[-\frac{2\pi^2}{3}\right.\\&-3\mathrm{Li}_2(x)-2\mathrm{Li}_2(-x)+\frac{7}{4}\ln^2(x)\\&-3\ln(x)\ln(1-x^2)-\frac{3}{4}\ln(x)\\&\left.+\frac{3}{2}\ln(x)\ln\left(\frac{s}{M_H^2}\right)\right],\end{aligned} \tag{47}$$

$$\begin{aligned}W_2(s)=&\frac{\pi^2}{6}+\frac{M_H^2}{2s}\ln\left(\frac{s}{M_H^2}\right)-\frac{1}{2}\left(1-\frac{M_H^2}{s}\right)\\&+\frac{1}{8}\ln^2\left(\frac{s}{M_H^2}\right)-\frac{3}{8}\ln^2(x).\end{aligned} \tag{48}$$

Here again, the variable x is defined by Eq. (24).

Performing the analytic continuation to the region $s<4M_H^2$, we find the expressions for the above integrals

$$W_1(s)+W_3(s)=\frac{1}{4}\left(1-\frac{M_H^2}{s}\right)-\frac{1}{8}\ln\left(\frac{s}{M_H^2}\right)+\frac{1}{8}\ln^2\left(\frac{s}{M_H^2}\right)-\frac{M_H^2}{2s}\ln\left(\frac{s}{M_H^2}\right)+\frac{\cot\left(\frac{\varphi}{2}\right)}{2}\left[\left(\varphi-\frac{\pi}{3}\right)\left(\frac{3}{4}-\frac{3}{2}\ln\frac{s}{M_H^2}+3\ln(2\sin(\varphi))\right)+\frac{1}{2}[3\mathrm{Cl}_2(2\varphi)-2\mathrm{Cl}_2(\varphi)]\right], \quad (49)$$

$$W_2(s)=\frac{M_H^2}{2s}\ln\left(\frac{s}{M_H^2}\right)-\frac{1}{2}\left(1-\frac{M_H^2}{s}\right)+\frac{1}{8}\ln^2\left(\frac{s}{M_H^2}\right)+\frac{3}{8}\left(\varphi-\frac{\pi}{3}\right)^2, \quad (50)$$

where φ is defined after Eq. (41). Equations (47)–(50) provide us with the desired result for the contribution of this graph to the imaginary part of $F(s)$.

The integration in the dispersion integral has to be done numerically and we find

$$F^{(13)}=-2\left(\frac{M_H}{4\pi v}\right)^2 K, \quad K=0.0678. \quad (51)$$

Summing up all contributions to the real part of $F(s)$ and taking into account permutations of the photon's legs where necessary, we obtain the final result

$$F=F^{(0)}+\sum_{i=1}^{6}F^{(i)}+2F^{(7)}+4F^{(8)}+4F^{(9)}+2F^{(10)}+2F^{(11)}+2F^{(12)}+4F^{(13)}=2\left[1-3.027\left(\frac{M_H}{4\pi v}\right)^2\right]. \quad (52)$$

The result [Eq. (52)] completes our calculation and presents the two-loop correction to the one-loop result [Eq. (2)].

IV. DISCUSSION AND CONCLUSIONS

Generally, it is not easy to say for which values of the Higgs boson mass our results (based on the application of the equivalence theorem) provide sufficiently accurate predictions for the value of the radiative correction. The only hint that can be obtained is from a comparison of the full one-loop result for the $H\gamma\gamma$ vertex with the result obtained by applying the equivalence theorem [Eq. (2)].

The complete one-loop result for the effective form factor $F(s)$ is plotted in Fig. 6. As mass parameters, we have taken $m_t=180$ GeV and $m_W=80$ GeV. Curve A shows the contribution of the W boson only, whereas curve B is the sum of the top quark and the W boson contributions. Figure 6 shows that the contribution of the W boson to $F(s)$ is slowly approaching its asymptotic value $F^{\mathrm{LO}}=2$ at $m_H>600$ GeV and

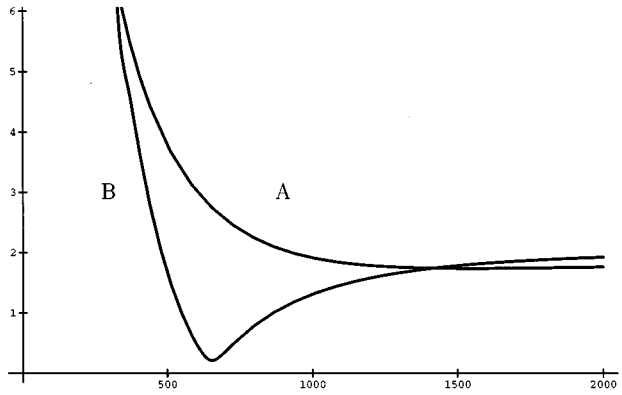

FIG. 6. Absolute value of the one-loop form factor $F(m_H)$ of process $H\to\gamma\gamma$ as a function of the Higgs boson mass M_H [GeV]. Curve A shows contribution of the W boson only, whereas curve B is the sum of the top quark and the W-boson contributions.

the contribution of the top quark is important until the Higgs boson mass reaches the value $m_H\sim 1$ TeV. We emphasize that there is a strong cancellation between the contributions of the top quark and W boson for Higgs boson masses of order $m_H\sim 600$ GeV.

Consequently, we expect that, in the two-loop case, the use of the equivalence theorem for an estimation of the electroweak (EW) radiative corrections for the coupling of the Higgs boson to two photons is reasonable for Higgs boson masses ≈ 600 GeV. Below this value, our results must be considered to be a rough estimate which have to be used in the absence of the exact calculation. It can also happen that some other potentially large SM radiative corrections (for instance, the ones proportional to top-Higgs-Yukawa coupling) should be taken into account to provide a more accurate estimate of the full SM radiative corrections for the Higgs boson masses below 1 TeV. Note that there are also large logarithmic contributions of powers of $\ln(M_H^2/m_W^2)$ to the subleading order $O(G_F m_W^2)$ which can reduce the range of validity for our result [Eq. (52)].

Our results for the leading two-loop EW corrections are presented in Fig. 7. We show the ratio of the leading two-

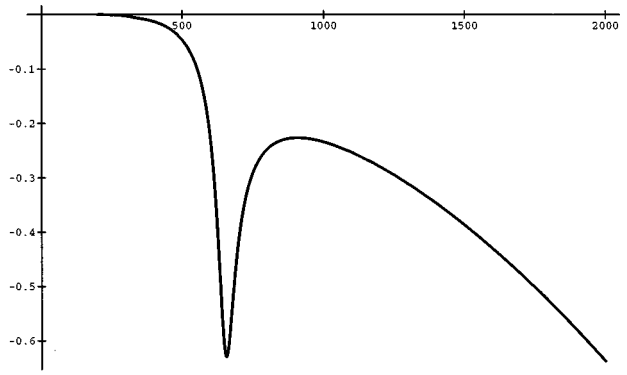

FIG. 7. Relative two-loop electroweak correction to the decay width $H\to\gamma\gamma$ (in percent) as a function of M_H [GeV].

loop electroweak correction to the $H\to\gamma\gamma$ decay width [see Eq. (52)] and the full one-loop result (W boson plus top contribution). One notes that the relative correction to the decay width is negative and large for $m_H>500$ GeV because of strong cancellations between W and top loops in the lowest order (see Fig. 6), but the absolute correction is small and perturbatively under control. This correction grows with the mass of the Higgs boson and blows up at around $m_H\sim 1.5$ TeV. This general behavior is quite familiar from previous studies of the large Higgs boson mass two-loop radiative corrections [14,15].

Finally, we want to comment on some phenomenological issues. A nice place for the investigation of the Higgs boson coupling to photons would be photon linear colliders, where the Higgs bosons would be produced through the reaction $\gamma\gamma\to H\to X$ [4]. The current limitations for the observation of the Higgs boson signal in this reaction is $M_H\leqslant 400$ GeV [16]. As was mentioned before, for such Higgs boson masses, our results should be considered only as an estimate of the full SM radiative corrections. However, they demonstrate that the SM correction is well under control in this mass range.

The heavy Higgs boson is a broad resonance with a width growing proportionally to M_H^3. It is evident that our results for the radiative correction to the on-shell value of the $H\gamma\gamma$ interaction vertex are not sufficient for the description of the Higgs boson shape in the reaction $\gamma\gamma\to H\to X$. However, since we have also given results for the imaginary part of the $H\gamma\gamma$ vertex, it is straightforward to obtain off-shell values for the $H\gamma\gamma$-vertex using dispersion integrals to evaluate the off-shell vertex numerically.

ACKNOWLEDGMENTS

We would like to thank J. Gasser for an informative discussion. J.G.K. and O.I.Y. were supported by the BMFT, FRG, under Contract No. 06MZ566. J.G.K., K.M., and O.I.Y. were supported in part by the Human Capital and Mobility program, EU, under Contract No. CHRX-CT94-0579. K.M. was supported by Graduiertenkolleg ''Teilchenphysik,'' Mainz.

[1] P. Janot, in *Neutrino 94*, Proceedings of the 16th International Conference on Neutrino Physics and Astrophysics, Eilat, Israel, edited by A. Dar *et al.* [Nucl. Phys. B (Proc. Suppl.) **38** (1995)].

[2] D.A. Dicus and V.S. Mathur, Phys. Rev. D **7**, 3111 (1973); B.W. Lee, C. Quigg, and H.B. Thacker, Phys. Rev. Lett. **38**, 883 (1977); Phys. Rev. D **16**, 1519 (1977); M. Veltman, Acta Phys. Pol. B **8**, 475 (1977); Phys. Lett. **70B**, 253 (1977).

[3] M. Lüscher and P. Weisz, Nucl. Phys. **B318**, 705 (1989); J. Kuti, L. Lin, and Y. Shen, Phys. Rev. Lett. **61**, 678 (1988); A. Hasenfratz, K. Jansen, J. Jersak, C.B. Lang, T. Neuhaus, and H. Yoneyama, Nucl. Phys. **B317**, 81 (1989); G. Bhanot and K. Bitar, Phys. Rev. Lett. **61**, 798 (1988); U.M. Heller, M. Klomfass, H. Newberger, and P. Vranas, Nucl. Phys. **B405**, 555 (1993).

[4] I.F. Ginzburg, in *Physics at LEP200 and Beyond*, Proceedings of the Workshop on Elementary Particle Physics, Teupitz, Germany, 1994, edited by T. Riemann and J. Blumlein [Nucl. Phys. B (Proc. Suppl.) **37B**, 303 (1994)]; P.M. Zerwas, in *Photon-Photon Collisions*, Proceedings of the International Workshop, Shoresh, Israel, 1988, edited by U. Kershon (World Scientific, Singapore, 1988).

[5] J. Ellis, M. Gaillard, and D.V. Nanopoulos, Nucl. Phys. **B106**, 292 (1976).

[6] M. Shifman, A. Vainstein, M. Voloshin, and V. Zakharov, Sov. J. Nucl. Phys. **30**, 1368 (1979).

[7] L.B. Okun, *Leptons and Quarks* (North-Holland, Amsterdam, 1982).

[8] A. Djouadi, M. Spira, J.J. van der Bij, and P.M. Zerwas, Phys. Lett. B **257**, 187 (1991); M. Spira, A. Djouadi, and P.M. Zerwas, *ibid.* **311**, 255 (1993); K. Melnikov and O. Yakovlev, Phys. Lett. B **312**, 179 (1993); K. Melnikov, M. Spira, and O. Yakovlev, Z. Phys. C **64**, 401 (1994).

[9] A. Djouadi and P. Gambino, Phys. Rev. Lett. **73**, 2528 (1994).

[10] J.M. Cornwall, D.N. Levin, and G. Tiktopoulos, Phys. Rev. D **10**, 1145 (1974); **11**, 972 (1975); M.S. Chanowitz and M.K. Gaillard, Nucl. Phys. **B261**, 379 (1985).

[11] See, for instance, S. Dawson, in *CP Violations and the Limits of the Standard Model*, Proceedings of the Theoretical Advanced Study Institute, Boulder, Colorado, 1994, edited by J. Donoghue (World Scientific, Singapore, 1995).

[12] A.D. Dolgov and V.I. Zakharov, Nucl. Phys. **B27**, 525 (1971).

[13] L. Lewin, *Polylogarithms and Associated Functions* (Elsevier, New York, 1981).

[14] J. Fleischer, O.V. Tarasov, and F. Jegerlehner, Phys. Lett. B **319**, 249 (1993).

[15] L. Durand, B. Kniehl, and K. Riesselmann, Phys. Rev. D **51**, 5007 (1995).

[16] G. Belanger, Talk delivered at the Photon '95 Conference, ENSLAPP-A-527/95, hep-ph/9508218 (unpublished).